 CMES, vol.71, no.1, pp.67-92, 2011

A New Molecular Structural Mechanics Model for the Flexural Analysis of Monolayer Graphene

G. Shi[1] **and P. Zhao**[1]

Abstract: Based on molecular mechanics and the concept of flexible connection used in the flexibly connected frames, a new structural mechanics model, a 2-D frame composed of anisotropic beams and flexible connections, is proposed for the simulation of the static and dynamic flexural behavior of monolayer graphene. The equivalent beam representing the C-C bond in the new molecular structural mechanics (MSM) model has two salient features compared with other MSM models presented for the analysis of carbon nanotubes: one is that the flexible connections at the beam ends are used to account for the bond-angle variations between the C-C bonds of graphene; and the other is that there are two principal flexural rigidities used for the flexible connections to reflect the different behaviors of the σ-bond and π-bond in the graphene lattice. The mechanical properties of the equivalent beam for the C-C bond of graphene lattice are evaluated from the force constants of graphene given by molecular mechanics. The in-plane Young's moduli, Poisson ratios, equivalent flexural rigidities and the flexural frequencies of monolayer graphene are simulated using the proposed new MSM model coupled with ANSYS. The simulation results show that the 2-D flexibly connected frame of the new MSM model proposed in this paper gives improved predictions of the in-plane Young's moduli, Poisson ratios and flexural rigidities of monolayer graphene than other MSM models. The present study also indicates that monolayer graphene is kind of an orthotropic material since both the in-plane elastic constants and the flexural rigidities of monolayer graphene are the principal directions dependent.

Keywords: Graphene, elastic constants, flexural rigidities, molecular mechanics, bond angle variation, flexible connection.

1 Introduction

Graphene is a monolayer of covalently bonded carbon atoms arranged in a honeycombed lattice. There are growing experimental and analytical evidences [Novoselov

[1] Department of Mechanics, Tianjin University, Tianjin 30072, China.

et al (2004); Lee et al (2008); Li and Kaner (2008); Geim (2009); Horing (2010) among others] indicating that monolayer graphene has exceptional physical properties such as nanoscale, low density, high modulus as well as high strength, and it also possesses extraordinary electronic, thermal, chemical, optical and other properties. The exceptional properties of graphene make it a 'device-friendly' material in various engineering applications. Because the monolayer graphene sheet forms the basis of one-dimensional (1-D) carbon nanotubes (CNTs), some mechanical properties of monolayer graphene had been studied [e.g. Kudin et al (2001); Odegard et al (2002); Li and Chou (2003)] even before the monolayer graphene was discovered [Novoselov et al (2004)].

The investigation of the mechanical properties of graphene is an essential step for the proper applications of graphene such as in Nano Electro-Mechanical Systems (NEMS), advanced composites with graphene reinforcements and other areas. The method of experimental measurements is of high cost, and the measured results are also highly scattered because the specimen size of graphene is too small to properly apply loads and boundary conditions. Although the method of the analytical analysis is relative cost-effective compared with the experimental method, it can only be applied to the graphene based materials with simple geometry and subjected to simple deformations modes. However, on the other hand, the computer-based numerical methods are powerful tools to simulate the mechanical properties of graphene based materials with various loading and boundary conditions.

The mechanical properties of a nano-structure composed of an atomic or a molecular cluster can be characterized by the atomic interactions in the nanoscale material. The two most common models used to describe these interactions in nanoscale materials are quantum mechanics and molecular mechanics. Both of these models attempt to capture the variation of the system energy associated with the changes of atomic positions. Quantum mechanics is rigorous and accurate as it determines the system energy based on calculations of the electronic structure of molecules, however it is very time-consuming even when simplifications are made (e.g., the semi-empirical methods). By using the Born–Oppenheimer approximation, molecular mechanics neglects the electronic structure as well motion of electrons and it expresses the system energy only as a function of the nucleus positions. A number of molecular mechanics-based models have been proposed for the analysis of CNTs in the past decade. Odegard et al (2002) proposed a pin-jointed truss model for CNTs; but more truss members in addition to the basic hexagonal cells of the C-C bonds of graphene have to be used in the truss model in order to make the equivalent truss of a carbon nanotube to be stable. Chang and Gao (2003) presented an accurate stick-spiral model for CNTs; however this model is only valid for the axial deformations analysis of CNTs or graphene. Li and Chou (2003) proposed

a molecular structural mechanics (MSM) model where CNTs are modeled by the equivalent rigidly connected frames and the inversion energy is not taken into account explicitly. Based on the MSM proposed by Li and Chou (2003), Li and Guo (2006) used the rectangular beams to account for the different bending behaviors of the in-plane bending and out-of-plane bending of a single layer graphite sheet; but the force constant for the out-of-plane bending is not accurate as it is evaluated from the equivalent flexural rigidity of the cylindrical shell of CNTs. Georgantzinos et al (2009) presented a linear spring based finite element formulation; theoretically this model is able to account for the bond angle variations, but this linear spring model is not computationally efficient since more structural members have to be used. Based on the MSM model of Li and Chou, Chen et al (2010) proposed a modified MSM model in which rectangular beams are also used to account for the different force constants for the in-plane bending energy and the inversion energy. However, this modified MSM model is not capable of accounting for the bond angle variation either as in the case of Li and Chou's MSM model, and furthermore the force constant used for the inversion energy in this modified MSM model in fact is for the improper torsion [Cornell et al (1995)].

CNTs or graphene can also be analyzed by their equivalent continuum mechanics models. The continuum mechanics models of isotropic cylindrical shells or isotropic plates are widely used [Odegard et al (2002); Huang et al (2006)]. There are two shortages in the isotropic shell model of CNTs or the isotropic plate model of graphene. Firstly it is not realistic to treat the CNTs or graphene as the continuums made of isotropic materials; secondly the determination of the proper representative thicknesses of CNTs and graphene is not straightforward as it was shown that the representative thickness of CNTs or graphene used to evaluate the stretching stiffness and flexural rigidity is much smaller than the inter-planar spacing of graphite layers [Yakobson et al (1996); Ru (2000)]. Moreover, the representative thicknesses of CNTs or graphene are not a constant but depending on the types of loading [Huang et al (2006)]. Theodosiou and Saravanos (2007) proposed a molecular mechanics based finite element for the analysis of CNTs, but this model can not take account of the bond angle variations properly.

All these different methods for the mechanical property analysis of CNTs or graphene could yield quite good in-plane Young's modulus or stretching stiffness of graphene where the variation among the different predicted results is about 6-11% [Wang and Zhang (2008)]. But the predicted Poisson ratios by different models are ranged from 0.06 [Li and Chou (2003); Chen et al (2010)] to 1.44 [Sakhaee-Pour (2009)], and the predicted flexural rigidity of CNTs are scattered from 0.69 eV to 3.28 eV [Wang and Zhang (2008)]. The fact that some analysis models are of capable of predicting reasonable good in-plane Young's modulus but resulting in unreason-

able Poisson ratios indicates that the deformation pattern predicted by these models might be incorrect.

The MSM model proposed by Li and Chou (2003) is quite computationally efficient. But the equivalent beams to represent the C-C bond in this model are rigidly connected to carbon nuclei, which results in that the bond angle variations of graphene can not be taken into account. All the modified or revised MSM models presented, respectively, by Li and Guo (2006), Sakhaee-Pour (2009), and Chen et al (2010) are not able to account for the bond angle variations either. As it will be shown later, the deformation pattern predicted by these MSM models with rigid connections are not accurate as the predicted lateral deformations is much smaller than the results predicted by other accepted models although the predicted longitudinal Young's modulus of CNTs or the in-plane Young's modulus of graphene given by these MSM models are quite good. Consequently, it can be concluded that the correct modeling of the bond angle variations for the C-C bonds of CNTs or graphene is very important for the accurate predictions of the mechanical properties of CNTs or graphene.

Both static and dynamic flexural responses are very important for the NEMS made of graphene. The resistance to the flexural motion, or called the flexural rigidity, of graphene sheets is contributed primarily from the π–bonds of carbon atoms. Therefore, an accurate modeling of the flexural rigidity of graphene is very critical for the accurate study of flexural responses of graphene-based materials. The computational chemistry shows that the π–bonds in the lattice made of sp^2 carbons is much weaker than its σ-bonds. Therefore, the force constant representing the mechanical property of the π–bond is smaller than the force constant denoting the mechanical property of the σ-bond. Unfortunately, all the MSM models mentioned above are not capable of correctly taking account of the force constant for the inversion energy attributed from the π–bonds of graphene although the rectangular beam element is used by Li and Guo (2006) as well as Chen et al (2010) respectively .

The objective of this paper is to propose a new MSM model for the simulation of the elastic properties as well as static and dynamic flexural behaviors of monolayer graphene. This new MSM model is of a planar frame composed of equivalent anisotropic beams and flexible connections [Shi and Atluri (1987, 1989)]. This new MSM model has two novel features compared with other MSM models proposed for the analysis of carbon nanotubes. The first one is that the equivalent beams representing the C-C bonds are flexibly connected to the nodes denoting the carbon nuclei to account for the bond-angle variations between any two nearest C-C bonds; and the second one is that two principal flexural rigidities for the flexible connections are used to respectively account for the in-plane bending behavior and the out-of-plane bending behavior of graphene in order to reflect the different mechan-

ical properties of the σ-bond and π-bond in the graphene lattice. The mechanical properties of the equivalent beam in the graphene lattice are evaluated from the force constants of the graphene lattice given by molecular mechanics. The in-plane Young's moduli, Poisson ratios, static flexural behavior and the flexural frequencies of monolayer graphene are simulated using the proposed new MSM model coupled with ANSYS. The simulation results show that the 2-D flexibly connected frame model of the new MSM proposed in this paper gives improved predictions of the in-plane Young's moduli, Poisson ratios as well as flexural rigidities of monolayer graphene compared with other MSM models proposed for the analysis of CNTs so far.

2 Molecular mechanics taking account of inversion energy explicitly

The basic concept in molecular mechanics is that the atomic interaction of a molecule can be described by a molecular force field. Molecular mechanics is a powerful and efficient model to characterize the interatomic potential and mechanical properties of a nanoscale material composed of an atomic or molecular cluster. In molecular mechanics, the interatomic potential energy of a molecule or an atomic lattice with arbitrary geometry is written as a sum of various two-body, three-body, and four-body interactions of valences plus some nonbonded interactions. Within small deformations, the total interatomic potential energy U_{total} of a molecular cluster can be expressed as the superposition of valence interactions and nonbonded interactions as [Rappe et al (1992); Cornell et al (1995)]:

$$U_{total} = U_r + U_\theta + U_\phi + U_\omega + U_{vdW} + U_{es} \tag{1}$$

where the first four terms are contributed from the valence interactions, and U_r, U_θ, U_ϕ and U_ω are the energies associated, respectively, with bond stretching, bond angle variation, dihedral torsional angle and inversion. The last two terms in Eq. (1) are contributed from the nonbonded interactions, U_{edW} is van der Waals term and U_{es} is electrostatic term, and these two energy terms can be neglected when the deformation is very small [Orgegard et al (2002); Chang and Gao (2003)].

For a carbon nanotube or monolayer graphene made of sp^2 carbon atoms, each valence interaction term in Eq. (1) takes the following form.

1) Bond stretching energy. There are many functional forms to define the bond stretching energy. When the deformation is small, the bond stretching energy U_r can be accurately written in a harmonic form as [Rappe et al (1992)]

$$U_r = \frac{1}{2}\sum_i K_r(\Delta r_i)^2 \tag{2}$$

where Δr_i is a bond elongation between two nearest atoms I and J as illustrated in Fig. 1a; K_r is the bond stretching force constant; and the summation is over all the C-C bonds in the monolayer graphene under consideration.

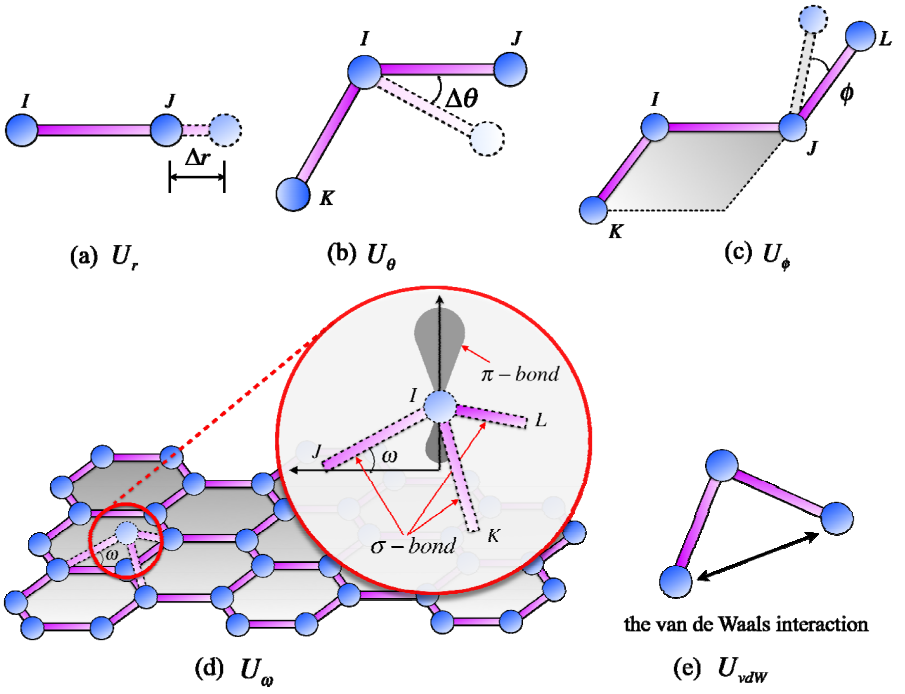

Figure 1: The energies of atomic interactions in molecular mechanics

2) Angle variation energy. The energy U_r induced by a bond angle variation can also be accurately expressed in a harmonic form when the deformation is small:

$$U_\theta = \frac{1}{2}\sum_j K_\theta (\Delta\theta_j)^2 \tag{3}$$

where $\Delta\theta_j$ is the bond angle variation between a bond IJ with bond IK, one of its nearest neighbor bonds, as depicted in Fig. 1b; K_θ is the bond bending force constant; and the summation is over all the bond angle variations in the system.

3) Torsional energy. The dihedral angle energy $U_\phi$is associated with the torsion of four-body interactions in an atomic system, and a typical torsion of such interactions is depicted in Fig. 1c. For the central bond IJ with both $I$and$J$ being sp^2 carbon atoms, U_ϕ is of the form [Rappe et al (1992)]

$$U_\phi = \frac{1}{2}\sum_k K_\phi (1 - \cos 2\phi_k) \tag{4}$$

where ϕ_k denotes the torsional angle of the central bond IJ of the corresponding four-body interactions as depicted in Fig. 1c; and K_ϕ is the bond torsional force constant. For small torsional angle, Taylor expansion leads to

$$U_\phi = \frac{1}{2}\sum_k K_\phi[1-(1-\frac{(2\phi_k)^2}{2}+\frac{(4\phi_k)^4}{4!}-...)] \approx \sum_k K_\phi \phi_k^2 \tag{5}$$

4) Inversion energy. The inversion energy $U_\omega$is associated with the interactions of an atom with its nearest three neighbor atoms in a molecule as shown in Fig. 1d. For a $C-2$ sp^2 carbon atom with exactly three substituents, U_ω is of the form [Rappe et al (1992)]

$$U_\omega = \sum_m K_\omega(1-\cos\omega_{IJKL}) \tag{6}$$

By using the orbital axis vector technique [Orgegard et al (2002)], the inversion angle variation ω_{IJKL} is defined the angle of the new location of atom I with respect to the plane formed by atoms J, K and L as depicted in Fig. 1d; and K_ω is the force constant for the inversion energy. Setting $\omega_m = \omega_{IJKL}$ for simplicity and using Taylor expansion for Eq. (5a), then under the assumption of small ω_m one has

$$U_\omega = \sum_m K_\omega[1-(1-\frac{\omega_m^2}{2}+\frac{\omega_m^2}{4!}-...)] \approx \frac{1}{2}\sum_m K_\omega \omega_m^2 \tag{7}$$

Equations (4b) and (5b) show that both the dihedral angle energy U_ϕ and the inversion energy U_ω can be expressed in the harmonic forms as long as the deformation of the molecular system under consideration is small.

3 A new molecular structural mechanics model for the mechanical property prediction of the lattice of monolayer graphene

A monolayer graphene sheet can be treated as a planar lattice comprised of hexagonal cells made of covalent bonds connected at carbon nuclei shown in Fig. 1d, which is analogous to the planar framed structures widely used in structure engineering. Therefore, the mechanical behavior of a monolayer graphene sheet could be studied by theory of structures. However, it should be noted that one special feature of the deformation pattern of a nanoscale carbon lattice is the bond angle variations shown in Fig. 1b, and in fact which is one of the major deformations in the lattices of graphene and CNTs when they are subjected to any external loading. Therefore, the modeling accuracy of the bond angle variations affects significantly the accuracy and reliability of any analysis model of carbon nanomaterials.

As mentioned in Introduction, the truss model [Odegard et al (2002)] and the linear-spring based model [Georgantzinos et al (2009)] are able to model bond angle variations, but they are not computational efficient; and furthermore, the establishment of their computational models is not straightforward since many additional structural members beyond the C-C bonds of graphene have to be used. The stick-spiral model [Chang and Gao (2003)] gives good axial Young's modulus of CNTs, but it is merely valid for the in-plane deformation analysis of graphene as the molecular potential in this model takes only the first two terms in Eq. (1). Although the rigidly connected frame model with the beams of circular cross-section proposed by Li and Chou (2003) is quite computationally efficient, it has two drawbacks. One is that the rigidly connected frame model can not characterize the bond angle variations, and the other is that the circular beam can not correctly model the inversion energy in Fig. 1d which is corresponding to the out-of-plane bending behavior of graphene. The modified MSM models presented respectively by Li and Guo (2006) as well as Chen et al (2010)) are not able to model the bond angle variations either because the rigid connections are used in these models. The new MSM model for the mechanical property prediction of the graphene lattice proposed in this paper aims to overcome aforementioned two drawbacks in the MSM model of Li and Chow (2003).

3.1 Flexible connection for the modeling of bond angle variation

The deformation pattern of the bond angle variations in the monolayer graphene depicted in Fig. 2a is very similar to that of the rotations taking place at junctions of flexibly connected frames comprised of rotational springs and beams with very large flexural rigidity shown in Fig. 2b where S_z denotes the rotational stiffness of the rotational spring defined in the $x-y$ plane of graphene. Therefore, the concept of the flexible connection in the flexibly connected frames [Shi and Atluri (1989)] can be used to model the bond angle variations in the lattice of graphene.

Shi and Atluri (1989) proposed an efficient computational model to characterize the behaviors of the nonlinear flexible connections in space-framed structures. The flexible connection model of Shi and Atluri (1989) will be used to model the bond angle variations of graphene in this study.

3.2 Flexural rigidity of the out-of-plane bending

As shown in Eqs. (5a) and (5b), the inversion energy of a graphene lattice is associated with the force constant K_ω that is different from the force constant K_θ related to the bond angle bending energy U_θ. As a result, the stiffness S_y of the rotational spring defined in the $x-z$ plane of the equivalent flexibly connected planar frame of graphene is different from S_z defined in the graphene plane. The inversion

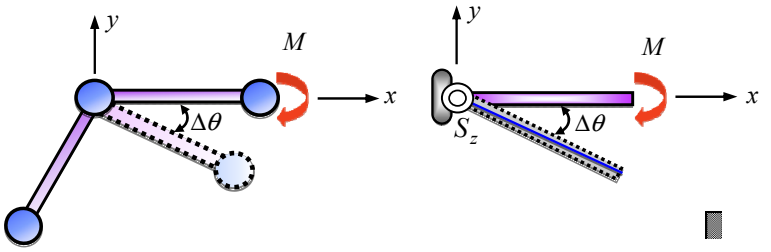

（a）bond angle variation (b) rotation at a flexible connection

Figure 2: Modeling of bond angle variation based on flexible connection

angle variation associated with the inversion energy can be modeled by a flexible connection of rotational stiffness S_y as illustrated in Fig. 3.

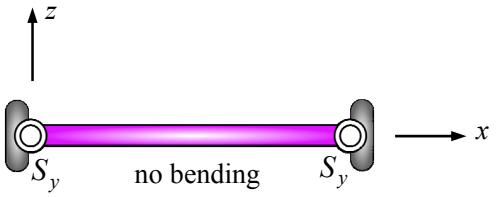

Figure 3: Modeling of the inversion angle variation associated with the inversion energy

3.3 The computational model given by the new molecular structural mechanics model

The basic idea illustrated by Figs. 2 and 3 is that a C-C bond of graphene can be treated as a load carrying structural member that is flexible in stretching and rotation, but stiff in bending and the all structural members are connected at the nuclei through the rotational springs. Consequently, the bond angle variations and inversion angle variations of a monolayer graphene sheet are characterized by the flexible connections at the nuclei of the graphene lattice. The computational model given by the new MSM model is illustrated in Fig. 4. It should be pointed out that the equivalent beam representing the C-C bond is of anisotropic and the mechanical properties of the equivalent beam is just characterized by its stretching stiffness EA,

rotational stiffness GJ and very large flexural rigidities both for in-plane bending and out-of-plane bending of graphene.

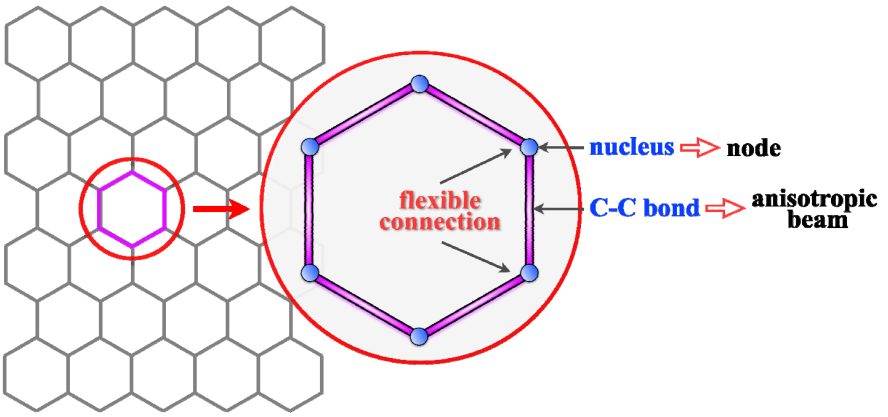

Figure 4: Computational model of graphene based on flexibly connected frame model

Shi and Atluri (1989) presented the element stiffness matrix of the beam with bonded rotational springs at the beam ends in the space-frame with nonlinear flexible connections. A constant axial force and twisting moment are assumed, while the linear bending moments in the two principal bending planes are interpolated in the stress-based space frame element presented by Shi and Atluri (1989). If let the force vector in the local coordinates of the C-C bond under consideration as $\mathbf{F}_{loc}$ where the bond axial axis is taken as the coordinate 1 and the normal of the graphene taken as the coordinate 3, then $\mathbf{F}_{loc}$ takes the form

$$\mathbf{F}_{loc} = \left\{N, M_1, {}^1M_2, {}^2M_2, {}^1M_3, {}^2M_3\right\}^T \tag{8}$$

in which N is the constant axial force acting on the beam; M_1 is the constant twisting moment; ${}^1M_2$ and ${}^2M_2$ are the bending moment around the coordinate 2 at node 1 and node 2 respectively, ${}^1M_3$ and ${}^2M_3$ are the bending moment around the coordinate 3 at node 1 and node 2 respectively. The corresponding nodal displacement vector $\mathbf{d}_{loc}$ is of the form

$$\mathbf{d}_{loc} = \left\{\Delta r, ({}^2\theta_1 - {}^1\theta_1), -{}^1\theta_2, {}^2\theta_2, -{}^1\theta_3, {}^2\theta_3\right\}^T \tag{9}$$

where Δr is the elongation of the C-C bond, ${}^\alpha\theta_i (i = 1,2,3,\ \alpha = 1,2)$ represent the rotation angle around the coordinate-i at node α.

Then, by assigning the beam representing the C-C bond with normal tensile stiffness EA and rotational stiffness EJ but with infinite flexural rigidities, Eq. (24) in the paper of Shi and Atluri (1989) leads the element stiffness matrix $\mathbf{K}_{loc}$ of an anisotropic beam with rotational springs at its ends defined in the C-C bond local coordinates as

$$\mathbf{K}_{loc} = \begin{bmatrix} EA/l & & & & & & \\ & EJ/l & & & & \mathbf{0} & \\ & & S_y & & & & \\ & & & S_y & & & \\ & \mathbf{0} & & & S_z & & \\ & & & & & S_z & \end{bmatrix} \tag{10}$$

where l is the C-C bond length, S_y and S_z are the stiffness of rotational springs as shown in Figs. 3 and 2 respectively. The beam stiffness matrix in the global coordinates can be evaluated by a normal transformation procedure widely used in the analysis of space frames [Shi and Atluri (1988)]. It is worthwhile to point out that the symbol EA in Eq. (8) is a single parameter used to denotes the equivalent tensile stiffness of a C-C bond, but not the product of the so-called cross-section area "A'' and the Young's modulus "E'' of the beam element for the C-C bond since a C-C bond only has a force constant K_r but no cross-section physically. The same is true for the rotational stiffness EJ in Eq. (8).

Shi and Atluri (1987, 1989) proposed two models to characterize the behaviors of the nonlinear flexible connection in space-framed structures. Among these two models, the model of the beam with bonded rotational springs at its ends shown in Fig. 5a is computational efficient, but this special beam element with the stiffness matrix given in Eq. (8) is not available in commercial FEA codes.

However on the other hand, the short flexible beam model for the equivalent rotational spring illustrated in Fig. 5b can be easily implemented into any existing finite element code. In this model, the main beam with flexibility in stretching and torsion but rigid in bending is connected to a junction of the framed structure by a short flexible beam where the flexural flexibility of the short beam is determined by the constraint to yield a equivalent rotational stiffness to the rotational spring.

3.4 The mechanical properties of the anisotropic beam for a C-C bond

Using the notations defined in Eqs. (6), (7) and (8), the stretching energy U_N, torsional energy U_{M_1}, in-plane bending energy U_{M_3} and out-of-plane bending energy U_{M_2} of an anisotropic beam bonded with a rotational spring at its ends are of the form

$$U_N = \tfrac{1}{2}\int_0^l \tfrac{N^2}{EA}dx = \tfrac{1}{2}\tfrac{N^2 l}{EA} = \tfrac{1}{2}\tfrac{EA}{l}(\Delta r)^2 \tag{11}$$

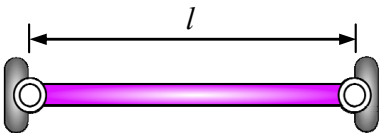

(a) rotational spring model

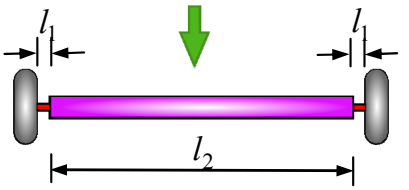

(b) flexible beam model

Figure 5: Two models for flexible connections of C-C bond

$$U_{M_1} = \frac{1}{2}\int_0^l \frac{M_1^2}{GJ}dx = \frac{1}{2}\frac{M_1^2 l}{GJ} = \frac{1}{2}\frac{GJ}{l}\phi^2 \tag{12}$$

$$U_{M_3} = \frac{1}{2}S_z(\Delta\theta)^2 \tag{13}$$

$$U_{M_2} = \frac{1}{2}S_y\omega^2 \tag{14}$$

It should be noted that there is no bending strain energy contributed from the main beam as it is rigid in bending.

When the rotational spring is represented by a short and highly flexible beam shown in Fig. 5b, the bond angle variation is also defined as the change of the angle between the two nearest bonds after the given deformation as shown in Fig. 1b. Then, the in-plane bending energy U_{M_3} in terms of the short flexible beam take the form

$$U_{M_3} = \frac{1}{2}\frac{D_z}{l_1}(\Delta\theta)^2 \tag{15}$$

where D_z is the flexural rigidity of the short flexible beam in the x-y plane and l_1 is the length the short flexible beam.

As illustrated in Fig. 1d, the inversion angle variation ω_{IJKL} at atom I is defined as the angle of the out-of-plane displacement of atom I with respect to the plane formed by its nearest three atoms J, L and L. When two short flexible beams used for the flexible connections, the inversion angle variation for bond IJ is defined by the angle between the line connecting atom I and atom J in the deformed configuration and the undeformed bond IJ as illustrated in Fig. 6. It can be seen from Fig. 6 that

the rotation angle taking place at each short flexible beam is a half of the inversion angle variation ω as in the case of the rotation angles at the two ends of a beam subjected to pure bending.

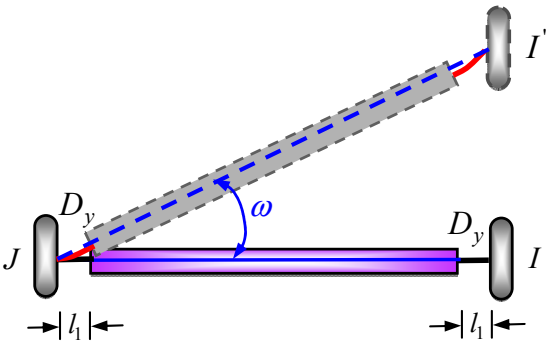

Figure 6: The inversion angle in the for the flexible beam model

Then the total out-of-plane bending energy U_{M_2} of the two flexible beams used to represent the flexible connections of a C-C bond is of the form

$$U_{M_2} = 2[\tfrac{1}{2}\tfrac{D_y}{l_1}(\tfrac{\omega}{2})^2] = \tfrac{1}{4}\tfrac{D_y}{l_1}\omega^2 \tag{16}$$

The strain energy of a beam in the equivalent framed structure of a graphene lattice evaluated from theory of structures should be equivalent to the molecular potentials of a C-C bond given by molecular mechanics. Consequently, the energy equivalence of a C-C bond defined by Eq. (2) to Eq. (5) and the strain energies expressed in Eq. (9) to Eq. (12) lead to

$$\frac{EA}{l} = K_r, \quad \frac{GJ}{l} = 2K_\phi \tag{17}$$

$$S_z = K_\theta, \quad S_y = K_\omega \tag{18}$$

The rotational stiffnesses given in Eq. (16) are the stiffnesses of the rotational springs in the rotational spring model. For the short flexible beam model shown in Fig. 5b and Fig. 6, both the main beam and the short beam have the same tensile and torsional stiffness as those in Eq. (15), but the flexural rigidities of the short flexible beam are given by

$$\frac{D_z}{l_1} = K_\theta, \quad \frac{D_y}{l_1} = 2K_\omega \tag{19}$$

Therefore, the mechanical properties of the equivalent anisotropic beam of a C-C bond can be determined provided that the force constants in Eq. (2) to Eq. (5) are given by molecular mechanics. And having obtained the mechanical properties of the rotational springs or the equivalent anisotropic beam, the mechanical properties of the equivalent flexibly connected frame of a graphene lattice can be evaluated by the general finite element procedure.

4 Results and discussion

4.1 Selection of force constants

The computational accuracy of the new MSM model presented in previous section strongly depends on the force constants used to characterize the mechanical properties of the equivalent beam for the C-C bond. Although quite a number of Potential Functions and Force Fields have been proposed in the past twenty years, little agreement has been reached in modeling the atomic bonds of graphite [Xiao and Hou (2006); Wang and Zhang (2008)], particularly the mechanical properties related to the inversion energy. For instance, different force constant K_r for bond stretching and force constant K_θ for bond angle variation were used, respectively, by Odegard et al (2002) aw well as Chang and Gao (2003).

The second generation force field AMBER developed by Cornell et al (1995) tabulates the molecular force constants for quite a wide range of organic molecules in condensed phases, but unfortunately the inversion energy was not explicitly included in AMBER. The bond stretching force constant K_r and bond angle variation force constant K_θ given by Cornell et al (1995) were employed by Odegard et al (2002) as well Li and Chou (2003) respectively, and they yield good axial Young's modulus of CNTs. The UFF (Universal Force Field) presented by Rappe et al (1992) is one of few Force Fields that describes explicitly the definition of the inversion energy U_ω, but the force constant K_ω for sp^2 carbons was only given by a general description in the paper of Rappe et al (1992). Nevertheless, one knows it from the chemical structure of sp^2 carbon molecule that the π–bonds in the lattice made of sp^2 carbon atoms is much weaker than its σ-bonds, and hence the force constant representing the mechanical property of the π–bond is smaller than the force constant denoting the mechanical property of the σ-bond. The force constants K_r, K_θ and K_ϕ given by Cornel et al (1995) and the force constants K_ω for the inversion energy given in a general statement by Rappe et al (1992) will be the first choice to be used in this study. These force constants take the following values

$$K_r = 938\frac{\text{kcal}}{\text{mol}}, \quad K_\theta = 126\frac{\text{kcal}}{\text{mol.rad}^2}, \quad K_\phi = 29\frac{\text{kcal}}{\text{mol.rad}^2}, \quad K_\omega = 6\frac{\text{kcal}}{\text{mol.rad}^2} \tag{20}$$

The bond stretching and bending force constants K_r and $K_\theta$in Eq. (18) are the same

as those used in the original MSM model of Li and Chou (2003), but the torsional force constant K_ϕ here is different from that used by Li and Chou. The authors believe that the torsional parameter $2 \times 14.5\text{kcal}/(\text{mol.rad}^2)$ for the sp^2 carbon given in Table 14 of the paper of Cornel et al (1995) is more suitable for graphene than the torsional parameters for other atom types in the same table. Since the second generation force field of Cornel et al (1995) does not include the inversion energy U_ω explicitly, the improper torsional energy in the resulting force constants of AMBER force field is not related to the inversion energy U_ω. Consequently, it is improper to use the dihedral parameter V_n listed for the improper torsional energy in the paper of Cornel et al (1995) for the force constant K_ω of the inversion energy.

4.2 The Young's moduli and Poisson ratios of graphene

In order to study the influence of graphene chirality on the in-plane Young's moduli, the Young's moduli of monolayer graphene along the two principal directions shown in Fig. 7 are evaluated. The length of C-C bond is taken as l= 0.142 nm in this study. As shown by Li and Chou (2003), the Young's moduli of a finite size monolayer graphene depend on the size of the computational models when there are only few atoms along its width. But the simulated Young's moduli of monolayer graphene converge to a constant value when the size of a monolayer graphene is large enough.

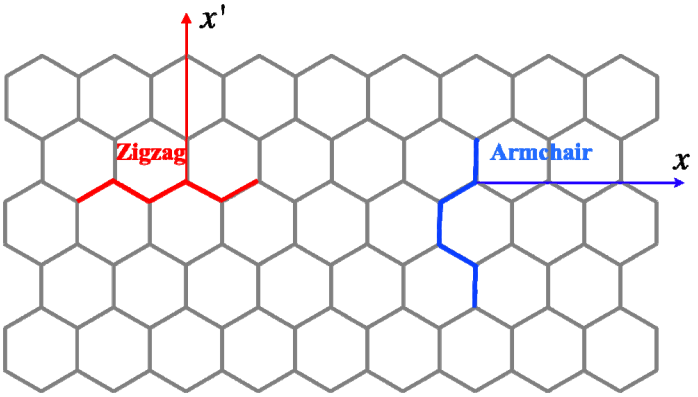

Figure 7: The honeycombed lattice of graphene C-C bonds

The Young's modulus of a zigzag monolayer graphene of size 8.378 nm $\times$ 19.553 nm and that of a armchair monolayer graphene of size 16.898 nm $\times$ 29.390 nm obtained from the present new MSM model are tabulated in Table 1. The results given by the original MSM model are also listed in the table for comparison.

Table 1: The Young's moduli and Poisson ratios of graphene given by different MSM models

Model	Zigzag		Armchair	
	Young's modulus (TPa)	Poisson ratio	Young's modulus (TPa)	Poisson ratio
present MSM model	1.004	0.237	1.141	0.201
original MSM model	1.033[a] 1.050[b]	– 0.086[b]	– 1.078[b]	– 0.078[b]

[a] the values given by Li and Chou (2003), size: 4.18 nm $\times$ 20.18 nm;
[b] the values computed by the authors based on Li and Chou's model.

Since Li and Chou (2003) only gave the Young's moduli of a zigzag graphite sheet with different sizes, all other elastic constants of the graphite sheets corresponding to the original MSM model in Table 1 are computed by the authors by reducing the present MSM model to the original MSM model.

The Young's moduli predicted by the present new MSM models shown in Table 1 or the corresponding tensile stiffness defined as the product of Young's modulus to the graphene thickness 0.34 nm agree well with the results given by other models (vide the summaries in the paper of Huang et al (2006)). The reported Poisson ratios of graphene given by different models are scattered in a wide range [Zhao and Shi (2011)]. The Poisson ratios of graphene predicted by the present MSM model agree with the Poisson ratios of CNTs with large diameters given by the majority of researchers [Zhao and Shi (2011)]. However, most of researchers only gave one value of Young's modulus since they treated the graphene as an isotropic material. The present results clearly indicate that both the Young's moduli and the Poisson ratios of monolayer graphene along the two principal directions of the graphene are different, that is the equivalent elastic constants of graphene are chirality dependent. The results in Table 1 also show that the Poisson ratios obtained from the original MSM model of Li and Chou (2003) are much smaller than the values given by the majority of researchers.

4.3 Influence of the modeling of bond angle variations

The predicted elastic constants of graphene in Table 1 show that the Poisson ratios obtained from the new MSM model with the flexible connection are totally different

from those given by the original MSM model with rigid connections, although the Young's moduli given by these two different MSM models are almost the same. The widely used Poisson ratio for graphite is 0.16 [Chang and Gao (2003)], and the majority of the predicted Poisson ratios of graphene is ranged from 0.15 [Kudin et al (2001)] to 0.41 [Huang et al (2006)]. The unreasonable smaller Poison ratios predicted by the original MSM model were confirmed by Chen et al (2010). Then a question can be raised, why does the present new MSM model and the original MSM models yield totally different Poisson ratios?

The present new MSM model takes the bond angle variation into account explicitly by the use of flexible connections, but the MSM model of Li and Chou (2003) does not account for the bond angle variations as it just equalizes the bending energy of the equivalent beam to the bond angle variation energy of the C-C bonds. Because the torsional and inversion force constants K_ϕ and K_ω have no influence on the behavior of in-plane deformation of graphene, then in the case of the in-plane elastic property prediction, the major difference between the present new MSM model and the MSM model proposed by Li and Chou (2003) just lies in the modeling of bond angle variations. Consequently, when the same bond stretching force constant K_r and angle variation force constant K_θ are used, the difference on the simulated in-plane elastic properties given by these two different MSM models can be attributed to the effect of the different modeling of bond angle variations in these two MSM models. The much smaller Poisson ratios of graphene predicted by the original MSM model means that the computational model of the rigidly connected planar frame yields a much smaller lateral deformation than the real lateral deformation of graphene lattice with bond angle variations, although this MSM model is able to predict a quite good longitudinal deformation. Consequently, it can be concluded that the unreasonable smaller Poison ratios obtained from the original MSM model indicate that the deformation pattern predicted by the framed structure with rigid connection is not correct. A framed structure with rigid connections means that the angles of all junctions in the frame are fixed at its undeformed configurations under any loading conditions. Therefore, it is obvious that the lateral deformation is constrained by the rigid connections where the angles of the hexagonal cells of graphene shown in Fig. 7 are kept as a fixed 120^0 whatever how large the axial deformation is.

4.4 Flexural rigidities of monolayer graphene

The flexural rigidity of monolayer graphene lattice is mainly contributed from the π–bonds of carbon atoms in the case of small deformation. Therefore, the force constant K_ω for the inversion energy is the dominant factor for the evaluation of the flexural rigidity of the equivalent plate of the graphene lattice. Since there is

no widely accepted force constant K_ω of the covalent bonds of graphite for the inversion energy, a value of $\frac{1}{6}K_\theta$ is also considered for K_ω in this study besides the value given in a general description in the paper of Rappe et al (1992). The flexural rigidities of the equivalent 2-D continuums of both zigzag and armchair monolayer graphene sheets predicted by the present new MSM model with different force constants for K_ω are tabulated in Table 2, where the values of the flexural rigidities are evaluated from the strain energy of the cantilevered-like plate subjected to a distributed bending moment at the opposite free edge. The flexural rigidities corresponding to the force constant for the improper torsional energy, which was used for K_ω in the paper of Chen et al (2010), are also listed in the table.

Table 2: The flexural rigidities of graphene given by different values of K_ω

force constant K_ω(kcal/mol)	**flexural rigidity D** (eV)	
	Zigzag	Armchair
6 [Rappe et al (1992)]	0.398	0.414
$K_\omega = \frac{1}{6}K_\theta$	1.393	1.449
$\frac{1}{3}$1.1[Chen et al (2010)]	0.0243	0.0253

The measured values of flexural rigidity of monolayer graphene are scattered widely because of the uncertainty of loading and boundary conditions applied on the nanoscale specimen of graphene. As a result, there is no agreement reached for the accurate value of the equivalent flexural rigidity of monolayer graphene up to now. The flexural rigidities of CNTs of different diameters predicted by various analysis models, including *ab initio* computations and molecular dynamics simulations, are ranged from 0.69 eV to 3.28 eV [Wang and Zhang (2008)]. For example, the flexural rigidity of a carbon nanotube of armchair chirality (7, 7) given by Yakobson et al (1996) is $D_{CNT} = 0.85$eV. The flexural rigidity of a monolayer graphene sheet is lower than that of the corresponding carbon nanotube. Therefore, the results in Table 2 show that the flexural rigidities of monolayer graphene predicted by the present MSM model based on the force constant K_ω for sp^2 carbons given by Rappe et al (1992) are in the correct range of the flexural rigidities of monolayer graphene. However, since the proper value of force constant K_ω for the inversion energy of graphene is still also an open question, the accuracy of the flexural rigidities of graphene shown in Table 2 can not be evaluated exactly. Nevertheless, the present MSM model is capable of predicting accurate flexural rigidities of monolayer graphene if the accurate force constant $K_\omega$is provided.

The predicted flexural rigidities in Table 2 also indicate that monolayer graphene should not be treated as an isotropic material in the flexural analysis since the flexural rigidities are also chirality dependent as in the case of in-plane elastic constants.

4.5 Flexural vibrations of monolayer graphene

If let $\{q\}$ and $\{\ddot{q}\}$ be, respectively, the global nodal displacement vector and the global nodal acceleration vector in the computational model of a graphene lattice, the equation of motion of an undamped monolayer graphene sheet takes the following form

$$[M]\ \{\ddot{q}\} + [K]\ \{q\} = \{0\} \tag{21}$$

where $[M]$ is the global mass matrix of the graphene lattice and $[K]$ is its global stiffness matrix. $[K]$ can be evaluated by the new MSM model presented in the previous section, and $[M]$ is a lumped mass matrix with a mass of carbon atom $m_c = 1.993 \times 10^{-26}$kg assigned only at the diagonal elements of $[M]$ corresponding to the translational degrees of freedom of the carbon nuclei in the graphene lattice. The eigenvalues of the equation of motion in Eq. (19) can be solved easily by any finite element code.

The frequencies of a monolayer graphene sheet depend on its geometry and boundary conditions. The natural flexural frequencies of the monolayer graphene sheets with the clamped-free and clamped-clamped boundary conditions are considered here. All the predicted frequencies are based on the force constant K_ω for sp^2 carbons given by Rappe et al (1992).

The fundamental flexural frequencies of a clamped–free monolayer of zigzag graphene as a function of aspect ratio L/W of length to width given by the present MSM model are plotted in Fig. 8. In order to reduce the influence of the atoms along the boundary of the graphene on the vibrational behavior, the width of the monolayer graphene is taken as *W=19.553* nm. The fundamental flexural frequencies of the monolayer graphene given by the present MSM model but with the equivalent rotational springs of circular flexible beams, i.e. $K_\omega = K_\theta$, are also displayed in the figure together with the frequencies evaluated from the original MSM model where circular beams are assumed for the C-C bonds and all beams are rigidly connected to the joints. The fundamental flexural frequencies of a clamped–clamped monolayer of zigzag graphene as a function of aspect ratio L/W given, respectively, by the present MSM model with two different force constants for K_ω and by the original MSM model are plotted in Fig. 9. It can be seen from Figs. 8 and 9 that the frequencies predicted by the original MSM model where a larger force constant for $K_\omega = K_\theta$ is used are higher than those predicted by the present new MSM model. When the same force constant $K_\omega = K_\theta$ is used for the inversion energy as in the case of the original MSM model, the present flexibly connected 2-D frame yields a little bit higher frequencies than the original MSM model. This is because the beams representing the C-C bonds of graphene in the flexibly connected 2-D frame

always keep straight and the out-of-plane bending is only localized at the areas near the nuclei of the graphene lattice, therefore the equivalent out-of-plane flexural rigidity of the 2-D frame composed of the bending free load carrying bars and flexible connections is stiffer than that of the 2-D frame with flexible beams and rigid connections.

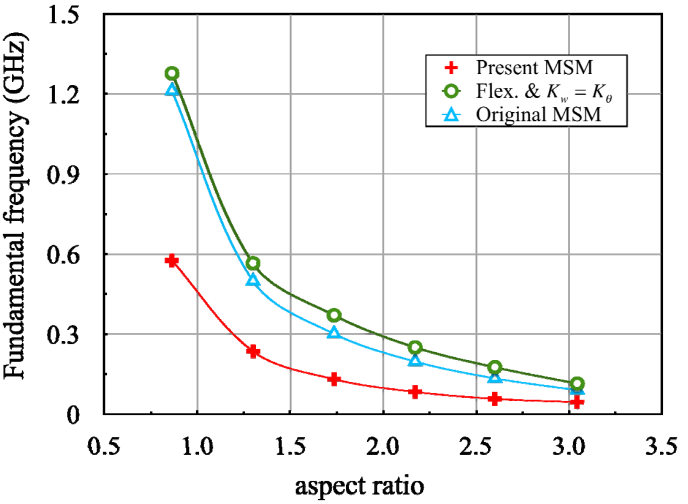

Figure 8: Fundamental flexural frequencies of lamped-free graphene as a function of aspect ratio W/L (zigzag, W=*19.553* nm)

There is very limited information on the frequency studies of graphene in the literature. The measured fundamental frequency of a suspended monolayer graphene sheet of W=1.93 μm and L=1.1 μm is 5.4 MHz [Bunch et al (2007)]. The frequency of the monolayer graphene sheet with size of 1.93 μm $\times$ 1.1 μm is too large to be solved by the MSM model in which each C-C bond is modeled as a load carrying structural member. Based on the MSM model of Li and Chou (2003), Hashemnia et al (2009) computed the fundamental flexural frequencies of monolayer graphene sheets, and the resulting frequencies of graphene are in the range of THz. The values of the frequencies given by Hashemnia et al (2009) seems too high for a monolayer graphene sheet since these fundamental flexural frequencies can match the fundamental flexural frequencies of CNTs with the same length reported by other researchers [e.g. Gibson et al (2007); Georgantzinos et al (2009)].

The higher vibrational modes are also important in many applications of graphene based devices and materials. The frequencies of the first 10 vibrational modes of a

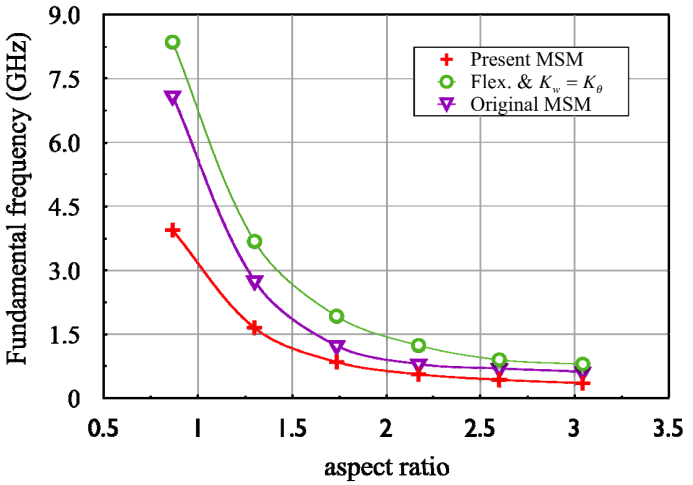

Figure 9: Fundamental flexural frequencies of clamped-clamped graphene as a function of aspect ratio W/L (zigzag, W=*19.553* nm)

clamped-free monolayer of armchair graphene predicted by the present new MSM model are plotted in Fig. 10. The dimension of the monolayer graphene is W=4.97 nm, L=*19.553* nm. The first 10 frequencies computed from the original MSM model are also given in the figure for comparison. The frequencies of the first 10 vibrational modes of a clamped-clamped armchair monolayer graphene obtained from the present new MSM model and the original MSM model are displayed in Fig. 11.

For both types of boundary conditions considered here, the frequencies of the first ten modes increase with the increase of the vibrational modes as expected. However, the frequency increase rate of the higher modes given by the present flexibly connected frame model is lower than that given by the rigidly connected frame because of the difference on the deformation pattern predicted by these different two MSM models.

5 Conclusions

Based on molecular mechanics and the concept of flexible connection, this paper presents a 2-D frame model composed of equivalent anisotropic beams and flexible connections, which is named as the new MSM model, for the static and dynamic flexural analysis of monolayer graphene. The equivalent beam representing the C-C bond in the new MSM model has two salient features compared with other

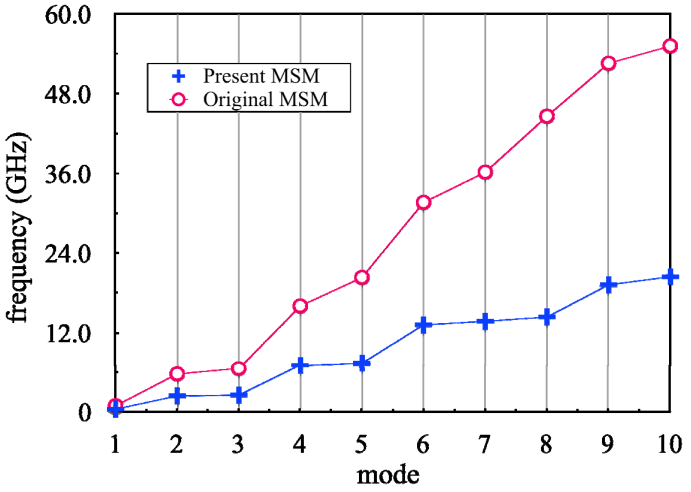

Figure 10: The frequencies of the first 10 modes of clamped-free armchair graphene (W=4.97 nm, L=*19.553* nm)

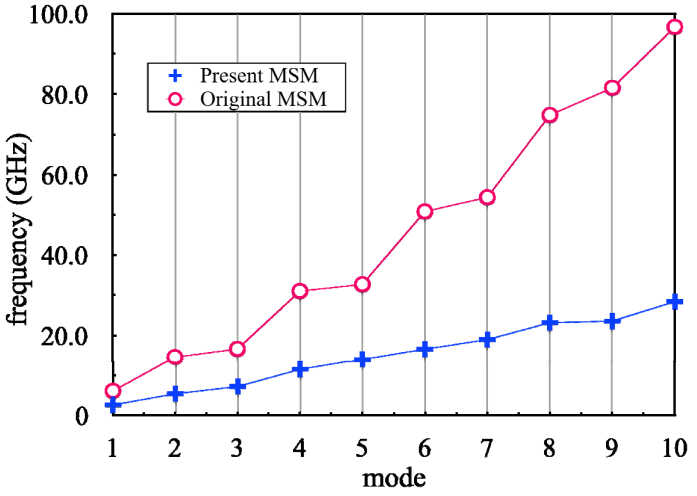

Figure 11: The frequencies of the first 10 modes of clamped-clamped armchair graphene (W=4.97 nm, L=*19.553* nm)

MSM models presented for the analysis of carbon nanotubes: the first one is that the bond-angle variations between the C-C bonds are taken into account by the

use of flexible connections; and the second one is that the force constant for the inversion energy that characterize the mechanical property of the π-bond in the graphene lattice is distinguished from the force constant associated with the bond angle variations controlled by the σ-bond in the graphene lattice. The mechanical properties of the equivalent anisotropic beam used for the C-C bond in the graphene lattice are evaluated from the force constants of the graphene given by molecular mechanics. The proposed new MSM model with short flexible beams can be easily implemented into any finite element code.

The in-plane Young's moduli and Poisson ratios as well the static flexural behavior and flexural frequencies of monolayer graphene are analyzed using the new MSM model coupled with ANSYS. The present MSM model gives the improved predictions of the in-plane Young's moduli, Poisson ratios as well as the equivalent flexural rigidities of monolayer graphene compared with other MSM models. Therefore, the 2-D flexibly connected frame model proposed in this paper is an accurate model to simulate the mechanical properties of graphene when the accurate force constants characterizing the atomic interactions of sp^2 carbon are provided. The following conclusions can be drawn from the present study.

1. The proper modeling of bond angle variation in the deformation of graphene is very important in the mechanical behavior simulations of graphene lattice, and the model of flexible connections is an efficient and accurate approach to characterize the bond angle variations of graphene lattice. For example, the present new MSM model in which a monolayer graphene is modeled as flexibly connected planar lattice predicts both accurate in-plane Young's moduli and good Poisson ratios for graphene, but the original MSM model in which a monolayer graphene is modeled as rigidly connected planar lattice yields much smaller Poisson ratios although it is able to predict quite good in-plane Young's moduli.

2. The force constant K_ω for the inversion energy that is used to characterize the mechanical property of the π-bond of graphene is the most important factor for the correct evaluation of the equivalent flexural rigidity of graphene since the flexural rigidity of a monolayer graphene sheet is contributed primarily from the π–bonds of carbon atoms. To date, there is limited study on the force constant K_ω of sp^2 carbons. Therefore, the investigation on the proper value of K_ω for graphene is very desirable.

3. Both the in-plane elastic constants and flexural rigidities of monolayer graphene predicted by the present MSM models suggest that a monolayer graphene sheet is a kind of orthotropic material as its mechanical properties along the two principal directions of graphene are different.

Acknowledgement: The financial support provided by the grants of NSFC-10872143

is thankfully acknowledged.

References

Bunch, J. S.; van der Zande, A. M.; Verbridge, S. S., et al (2007): Electromechanical resonators from graphene sheets. *Science,* vol. 315, pp. 490-493.

Chang, T.; Gao, H. (2003): Size-dependent elastic properties of a single-walled carbon nanotube via a molecular mechanics model. *J. Mech. Phys. Solids*, vol. 51, pp. 1059-1074.

Chen, W-H; Cheng, H-C; Liu, Y-L (2010): Radial mechanical properties of single-walled carbon nanotubes using modi?ed molecular structure mechanics. *Comput. Mater. Sci*., vol. 47, pp. 985-993.

Cornell, W. D.; Cieplak, P.; Bayly, C. I. et al (1995): A second generation force field for the simulation of proteins, nucleic acids, and organic molecules. *J. Am. Chem. Soc*., vol. 117, pp. 5179-5197.

Geim, A. K. (2009): Graphene: status and prospects. *Science,* vol. 324, pp. 1530-1534.

Georgantzinos, S. K.; **Giannopoulos, G. I**.; **Anifantis, N, K.** (2009): An efficient numerical model for vibration analysis of single-walled carbon nanotubes. *Comput. Mech*., vol. 43, pp. 731-741.

Gibson, R. F.; Ayorinde, E. O.; Wen, Y-F. (2007): Vibrations of carbon nanotubes and their composites: A review. *Composites Sci. & Tech.*, vol. 67, pp. 1-28.

Hashemnia, K.; Farid, M.; Vatankhah, R. (2009): Vibrational analysis of carbon nanotubes and graphene sheets using molecular structural mechanics approach. *Comput. Mater. Sci*., vol. 47, pp. 79-85.

Horing, N. J. M. (2010): Aspects of the theory of graphene. *Phil. Trans. R. Soc. A*., vol. 368, pp. 5525-5556.

Huang, Y.; Wu, J.; Hwang, K. C. (2006): Thickness of graphene and single-wall carbon nanotubes. *Physical Review B*, vol. 74, 245413.

Kudin, K. N.; Scuseria, G. E.; Yakobson, B. I (2001): C_2F, BN, and C nanoshell elasticity from *ab initio* computations. *Physical Review B*, vol. 64, 235406.

Lee, C.; Wei, X.; Kysar, J. W.; Hone, J. (2008): Measurement of the elastic properties and intrinsic strength of monolayer graphene. *Science*, vol. 321, pp. 385-388.

Li, C. Y.; Chou, T. W. (2003): A structural mechanics approach for the analysis of carbon nanotubes. *Int. J. Solids Struct.*, vol. 40, pp. 2487-2499.

Li, D.; Kaner, R. B. (2008): Graphene-based materials. *Science,* vol. 320, pp.

1170-1171.

Li, H.; Guo, W. (2006): Finite element model with equivalent beam elements of single walled carbon nanotubes. *Chinese J. Theor. Appl. Mech*., vol. 38, pp. 488-495. (in Chinese)

Lu, Q.; Arroyo, M.; Huang, R. (2009): Elastic bending modulus of monolayer graphene. *J. Physics D: Appl. Phys.*, vol. 42, 102002.

Novoselov, K. S.; Geim, A. K.; Morozov, S. V. et al (2004): Electric field effect in atomically thin carbon films. *Science,* vol. 306, pp. 666-669.

Odegard, G. M.; Gates, T. S.; Nicholson, L. M.; Wise, K. E. (2002): Equivalent-continuum modeling of nano-structured materials. *Composites Sci. & Tech.*, vol. 62, pp. 1869-1880.

Rappe, A. K.; Casewit, C. J.; Colwell, K. S. et al (1992): UFF, a full periodic table force field for molecular mechanics and molecular dynamics simulations. *J. Am. Chem. Soc*., vol. 114, pp. 10024-10039.

Ru, C. Q. (2000): Effective bending stiffness of carbon nanotubes. *Physical Review B*, vol. 62, pp. 9973-9976.

Sakhaee-Pour, A. (2009): Elastic properties of single-layered graphene sheet. *Solid State Commun.*, vol. 149, pp. 91-95.

Shi, G.; Atluri, S. N. (1987): Plastic-hinge analysis of flexible-jointed frames using explicitly derived tangent stiffness matrices. *Proc.6th OMAE*, Houston, Texas, pp. 393-401.

Shi, G.; Atluri, S. N. (1988): Elasto-plastic large deformation analysis of space frames: A plastic-hinge and stress-based explicit derivation of tangent stiffness. *Int. J. Num. Meth. Eng*., vol. 26, pp. 589-615.

Shi, G.; Atluri, S. N. (1989): Static and dynamic analysis of space frames with non-linear flexible connections. *Int. J. Num. Meth. Eng.*, vol. 28, pp. 2635-2650.

Theodosiou, T. C.; Saravanos, D. A. (2007): Molecular mechanics based finite element for carbon nanotube modeling. *CMES: Computer Modeling in Engineering & Sciences*, vol. 19, pp. 121-134.

Wang, C, Y.; Zhang, L. C. (2008): A critical assessment of the elastic properties and effective wall thickness of single-walled carbon nanotubes. *Nanotechnology*, vol. 19, pp. 1-5.

Xiao, S.; Hou, W. (2006): Studies of size effects on carbon nanotubes' mechanical properties by using different potential functions. *Fullerenes Nanotubes & Carbon Nanostruct*., vol. 14, pp. 9-16.

Yakobson, B. I.; Brabec, C. J.; Bernholc, J. (1996): Nanomechanics of carbon

nanotubes: instabilities beyond linear response. *Physics Review Letters*, vol. 76, pp. 2511-2514.

Zhao, P.; Shi, G. (2011): Study of Poisson ratios of graphene and single-walled carbon nanotubes based on an improved molecular structural mechanics model. *ICCES'11-Nanjing* (to appear).